Structural and impedance studies of copper-enriched (Cu$_{0.75}$Ag$_{0.25}$)$_7$SiS$_5$I-based ceramics

I.P. Studenyak[1], A.I. Pogodin[1], I.A. Shender[1], S.M. Bereznyuk[1], M.J. Filep[1], O.P. Kokhan[1], P. Kopčanský[2]

[1]*Uzhhorod National University, Faculty of Physics,*
3, Narodna Sq., 88000 Uzhhorod, Ukraine
[2]*Institute of Experimental Physics, Slovak Academy of Sciences*
47, Watsonova str., 04001 Košice, Slovakia
E-mail: studenyak@dr.com

Abstract. Copper-enriched (Cu$_{0.75}$Ag$_{0.25}$)$_7$SiS$_5$I-based ceramics were prepared from the micro- and nanopowders by pressing and sintering under developed technological conditions. Structural studies at different process step stages of ceramic samples preparation were performed using the XRD technique and microstructural analysis. The frequency and temperature dependences of the total electrical conductivity for (Cu$_{0.75}$Ag$_{0.25}$)$_7$SiS$_5$I-based ceramics were investigated by the impedance measurements. From the Nyquist plots, by using the electrode equivalent circuits the ionic and electronic components of the total electrical conductivity were determined. It has been shown that both ionic and electronic conductivity nonlinearly depend on the average crystallites size of (Cu$_{0.75}$Ag$_{0.25}$)$_7$SiS$_5$I-based ceramics.

Keywords: argyrodite, superionic conductor, ceramic, ionic conductivity, activation energy.

1. Introduction

Cu$_7$SiS$_5$I and Ag$_7$SiS$_5$I compounds with argyrodite structure are characterized by high ionic conductivity and thus belong to the superionic conductors or solid electrolytes that are the promising materials for different electrochemical (all-solid-state batteries, supercapacitors, ion-selective membranes, *etc*.) devices [1-3]. Electrical properties of (Cu$_{1-x}$Ag$_x$)$_7$SiS$_5$I mixed crystals were studied in Ref. [4]. It was shown that with Ag atoms content increase in (Cu$_{1-x}$Ag$_x$)$_7$SiS$_5$I mixed crystals the nonlinear increase of electrical conductivity from 0.003 S/cm (Cu$_7$SiS$_5$I) to 0.008 S/cm (Ag$_7$SiS$_5$I) is observed, as well as the ratio of ionic conductivity to the electronic one is nonlinearly increased by almost five orders of magnitude [4].

Recently, the composites [5, 6], ceramics [7] and thin films [8] based on the copper-containing argyrodites were investigated. In this paper, we focused on superionic ceramics studies. Nowadays, research on superionic ceramic materials related to the study and improvement of electrochemical energy storage technologies has been significantly promoted [9]. The active improvement of this technology is caused by the development of alternative energy sources and electric vehicles, as well as the growth of the number of portable electronic devices [10]. The supercapacitors, batteries and fuel cells are used as electrochemical energy storage devices [9]. Li-ion batteries containing liquid organic electrolyte have become the most commercially widespread [11]. However, the combination of chemically active lithium and flammable liquid reduces the safety of the device [12]. When using a solid electrolyte instead of a liquid electrolyte, it is possible to increase the safety of batteries, as well as to simplify its design [10, 13, 14].

Thus, in this paper we report on the preparation process and investigations of electrical conductivity of copper-enriched (Cu$_{0.25}$Ag$_{0.75}$)$_7$SiS$_5$I-based superionic ceramics.

2. Experimental

(Cu$_{0.75}$Ag$_{0.25}$)$_7$SiS$_5$I solid solution crystallizes in the face-centered cubic cell of argyrodite structure ($F\overline{4}3m$, $Z=4$) [2] with the lattice parameters $a = 9.9974(6)$ Å. Formation of the above-mentioned solid solution occurs due to the isostructure of Cu$_7$SiS$_5$I and Ag$_7$SiS$_5$I compounds and close ionic radii values (0.98 Å for Cu$^+$ and 1.13 Å for Ag$^+$) [15]. Clarification of the Cu$^+ \leftrightarrow$ Ag$^+$

substitution mechanism and coordinates of atoms in the cell was carried out on the basis of refined models of initial structures by using the Rietveld method [16, 17]. Calculation and refinement of the model was carried out using the program EXPO 2014 [18, 19], and visualization was performed using the program VESTA 3.5.2 [20]. The basis of the anionic framework of $(Cu_{0.75}Ag_{0.25})_7SiS_5I$ solid solution is constituted by $[SiS_4]$ (Fig. 1a), $[S_3I]$ and $[SI_4]$ tetrahedra that form icosahedra (Fig. 1b). The icosahedra are coordinated around the sulfur atom S1(4a), which is simultaneously the vertex of $[SiS_4]$ tetrahedra. Since the presence of interpenetrating icosaedera is characteristic of the structure of argyrodite, S1 is also the vertex of the next $[SS_9I_3]$ icosahedron. In the structure of $(Cu_{0.75}Ag_{0.25})_7SiS_5I$ the tetrahedron $[SiS_4]$ (Fig. 1a) is symmetrical (absolutely central Si position), the lengths of the Si–S bonds are 1.958Å, the distances S–S are 3.198 Å, the volume of tetrahedron is equal to 3.86 Å^3. Additionally, one can distinguish double tetrahedra $[Cu(Ag)S_3I_2]$ formed by sulfur atoms S1, S2 and atom I1 in the icosahedron (Fig. 1b). These doubled polyedra are coordinated around Cu1Ag1 and Cu2Ag2 substitution positions, from which a movable cationic sublattice of $(Cu_{0.75}Ag_{0.25})_7SiS_5I$ solid solution is formed.
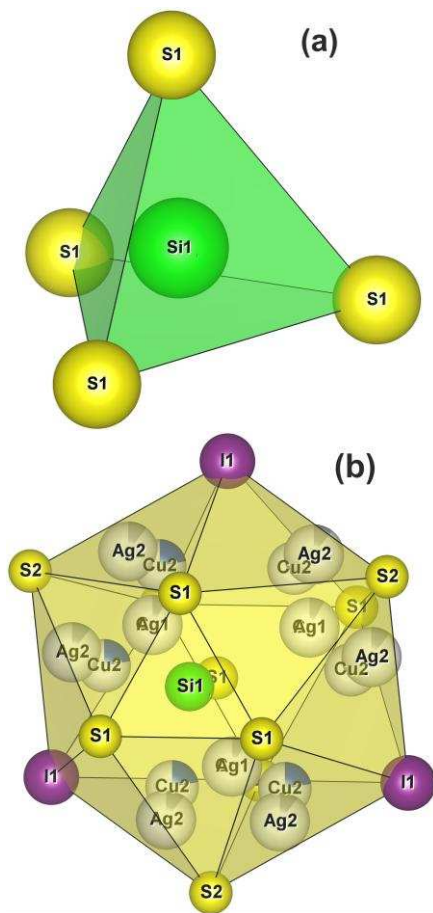
$(Cu_{0.75}Ag_{0.25})_7SiS_5I$ compound was synthesized by a direct single-temperature method from pre-synthesized quaternary Cu_7SiS_5I and Ag_7SiS_5I [4]. Microcrystalline powders were grinded in an agate mortar (average particle size of ~10…50 μm) as well as nanocrystalline powders were grinded in a planetary ball mill PQ-N04 for 30 and 60 min. XRD studies of micro- and nanopowders (DRON 4-07 with CuKα radiation, angle scanning speed 2θ–0.02 deg, exposure – 1 s) have shown that the argyrodite structure is preserved and the broadening of lines occurs when the particle size decreases (Fig. 2). SEM-studies have shown that the average particle size for powders grinded in the planetary ball mill for 30 min is ~150 nm, while at 60 min it is equal approximately 100 nm.

$(Cu_{0.75}Ag_{0.25})_7SiS_5I$-based ceramic samples were obtained by pressing the powders (at a pressure close to 400 MPa) and further sintering at 973 K for 36 hours in the form of disks with a diameter of 8 mm and thickness of 3-4 mm. The microstructural analysis of ceramic samples was performed with metallographic microscope METAM-R1. The microstructures and histograms of crystallites size distribution for different types of ceramics have been presented in Fig. 3. It is revealed that the average size of crystallites for ceramics obtained from microcrystalline powder is ~12 μm, and from nanocrystalline powders obtained by grinding for 30 and 60 min is ~5 µm and ~ 3 µm, respectively.
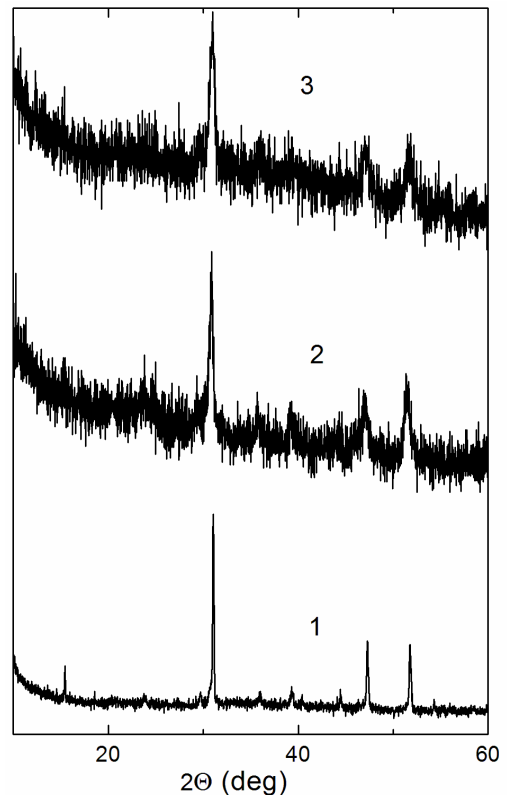

Fig. 1. $[SiS_4]$ tetrahedra (a) and $[SS_9 I_3]$ icosahedron (b) in the structure of $(Cu_{0.75}Ag_{0.25})_7SiS_5I$ solid solution.

Fig. 2. Diffractograms of $(Cu_{0.75}Ag_{0.25})_7SiS_5I$ powders obtained by grinding in agate mortar (*1*) and planetary ball mill for 30 min (*2*) and 60 min (*3*).
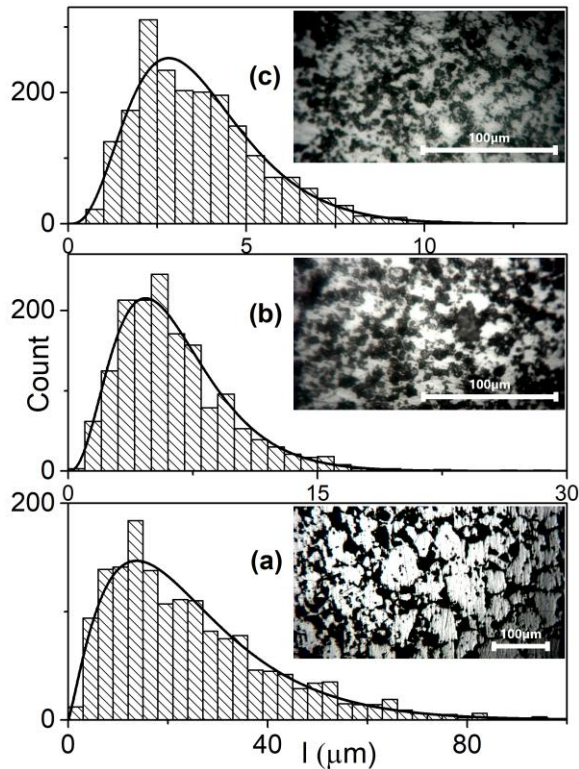
Studenyak I.P., Pogodin A.I., Shender I.A. et al. Structural and impedance studies of copper-enriched…

Fig. 3. Dependences of the size distribution for crystallites of $(Cu_{0.75}Ag_{0.25})_7SiS_5I$-based ceramics, obtained from powders that were milled in agate mortar (a) and planetary ball mill for 30 min (b) and 60 min (c). The inserts show the microstructure images for different $(Cu_{0.75}Ag_{0.25})_7SiS_5I$-based ceramics.

The electrical conductivity of $(Cu_{0.75}Ag_{0.25})_7SiS_5I$-based ceramics was measured with combination of high-precision LCR meters (Keysight E4980A and AT-2818) within the frequency range from 10 Hz to 2×10^6 Hz and temperature range from 292 up to 383 K. Measurement was carried out using the two-electrode method, with blocking (electronic) gold contacts deposited by chemical precipitation from solutions [4].

3. Results and discussion

The frequency dependences of the total electrical conductivity for $(Cu_{0.75}Ag_{0.25})_7SiS_5I$-based ceramics have been presented in Fig. 4. They are typical for solids with ionic conductivity: increase with a frequency, as it was observed [21]. The insert to Fig. 4 shows the dependence of the total electrical conductivity on the average crystallites size for $(Cu_{0.75}Ag_{0.25})_7SiS_5I$-based ceramics at the frequency 100 kHz. It has been shown that decrease of the average crystallites size from 12 μm down to 5 μm leads to increase of the total electrical conductivity by 22%, while the further decrease to 3 μm leads to decrease of the total electrical conductivity by 62%.

Being based on the Nyquist plots (Fig. 5) and using electrode equivalent circuits (EEC) [21-23], the total electrical conductivity of $(Cu_{0.75}Ag_{0.25})_7SiS_5I$-based ceramics was separated into ionic and electronic components. Three semicircles are observed on $Z'–Z''$

dependences for ceramic samples with average crystallites sizes close to 12, 5, and 3 μm. It has been shown that $(Cu_{0.75}Ag_{0.25})_7SiS_5I$-based ceramics is characterized by the predominance of the electronic component of electrical conductivity ($\sigma_{ion} < \sigma_{el}$). EEC selected for the description of the Nyquist plots can be separated into two parts: ionic that corresponds to the processes associated with the ionic component of conductivity and electronic one that corresponds to the electronic conductivity, respectively.

The low-frequency semicircles represent the diffusion relaxation processes at the electrode/crystal boundary, which is expressed by the included capacity of the double diffusion layer C_{dl} (Fig. 5). The parts of the structure with parameters R_{gb}/C_{gb} are series-connected to C_{dl} and responsible for the appearance of the "smeared" mid-frequency semicircle as well as characterize the resistance and capacity of the grain boundaries of the ceramic material. The high-frequency semicircles, in their turn, characterize conduction processes at intra-grain boundaries, which are described by the series-connected resistance R_{db} with the parallelly connected capacitance C_{db} (Fig. 5b, 5c). In the case of $(Cu_{0.75}Ag_{0.25})_7SiS_5I$-based ceramic sample with the average crystallite size of 12 μm, the high-frequency semicircle corresponds to the series-connected resistance of micro-grain R_d with the abovementioned parameters of R_{db}/C_{db} (Fig. 5a). Thus, the ionic conductivity of $(Cu_{0.75}Ag_{0.25})_7SiS_5I$-based ceramics is determined by the sum of the resistance of grain boundaries R_{gb} with resistance of intra-grain boundaries R_{db} and micro-grains resistance R_d (for the sample with the average crystallite size of 12 μm).

In parallel to the ionic processes, the electronic resistance R_e is included in the EEC, which contributes to the representation of all available semicircles on the Nyquist plots and determines the electronic component of the total electrical conductivity (Fig. 5).
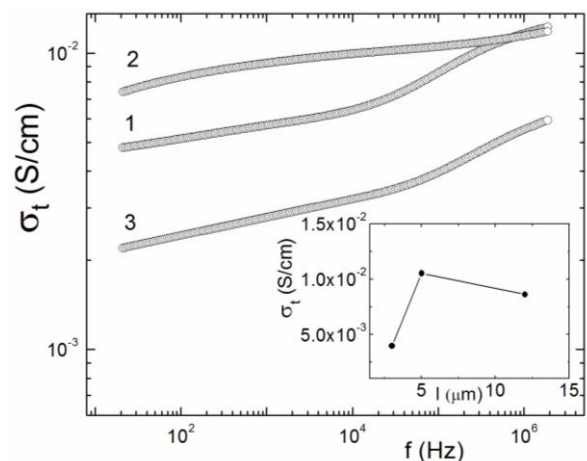

Fig. 4. Frequency dependences of total electrical conductivity at T = 298 K for $(Cu_{0.75}Ag_{0.25})_7SiS_5I$-based ceramics with different sizes of crystallites: 12 μm (*1*), 5 μm (*2*), 3 μm (*3*). The insert shows the dependence of the total electrical conductivity on the size of crystallites at 100 kHz.
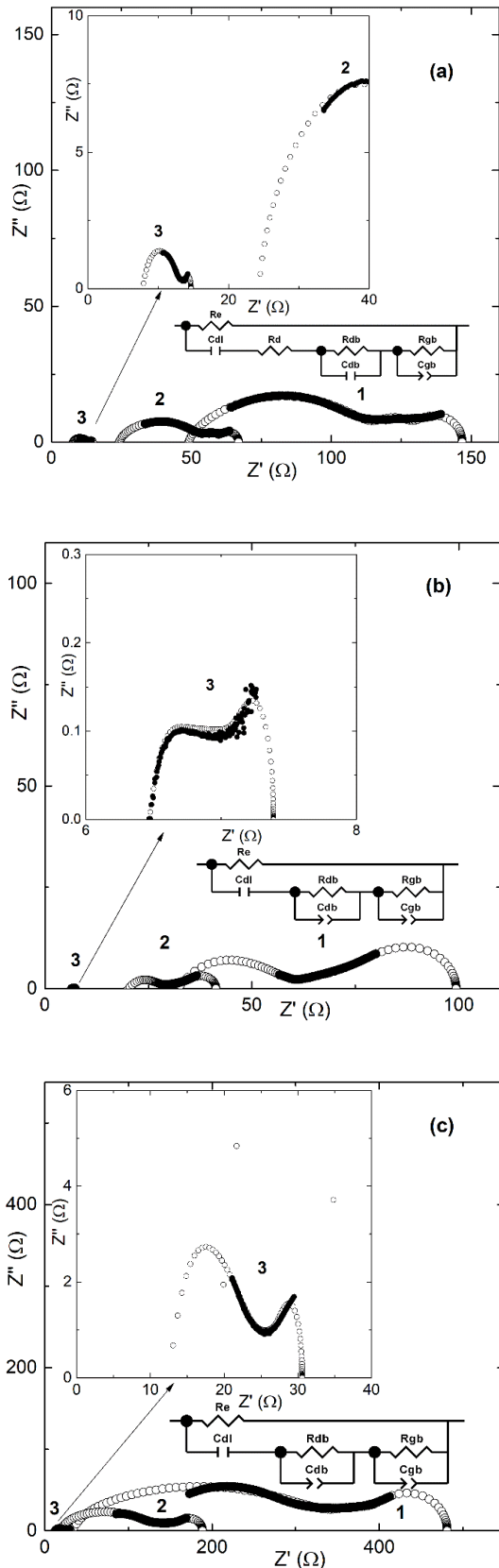
Studenyak I.P., Pogodin A.I., Shender I.A. et al. Structural and impedance studies of copper-enriched…

262

Fig. 5. EEC and Nyquist plots for $(Cu_{0.75}Ag_{0.25})_7SiS_5I$-based ceramics with different crystallite sizes: (a) 12 μm; (b) 5 μm; (c) 3 μm for temperatures 298 (1), 323 (2), 373 K (3). Experimental data correspond to the solid dots, calculated data correspond to the open dots.

In the analysis of Nyquist plots in the context of reducing the crystallites size from 12 μm down to 5 μm and further to 3 μm, the insignificant dynamics of the low-frequency semicircle shift into the low-frequency region is remarkable, which may be due to the preservation of the ratio $\sigma_{ion} < \sigma_{el}$, which together with high specific values of the electron component of electrical conductivity, defines practically equal influence of diffusion and relaxation ionic processes for samples of different dispersion.

Let us consider temperature evolution of Nyquist plots for $(Cu_{0.75}Ag_{0.25})_7SiS_5I$-based ceramics. With increasing the temperature, the increase of electronic conductivity is observed, which gradually eliminates the influence of diffusion ionic processes at the crystallite boundaries. It is accompanied by the decrease of the high-frequency semicircle at 323 K (Fig. 5, curve *2*). With the further increase of temperature up to 373 K (Fig. 5, curve *3*), there observed is a further decrease in the influence of diffusion ionic processes, which together with the decrease of thickness of double diffusion layer eventually leads to complete disappearance of mid-frequency semicircle and significant reduction of the high-frequency semicircle size, which is especially noticeable for ceramics with average crystallite size of 5 μm (Fig. 5b, curve *3*).

Fig. 6 shows the dependences of ionic and electronic components of electrical conductivity on the average crystallites size in $(Cu_{0.75}Ag_{0.25})_7SiS_5I$-based ceramics. It is revealed that reduction of average crystallite size down to 5 μm leads to the increase of both ionic (by 35%) and electronic (by 36%) components of electrical conductivity, whereas with further decrease of average crystallite size down to 3 μm, there is a sufficiently significant decrease of both ionic (by 61%) and electronic (by 75%) components of electrical conductivity. Such main characteristics of superionic materials as the ratio of ionic to electronic conductivity remains unchanged with decreasing the average crystallite size from 12 μm down to 5 μm and increases (by 57%) with decrease of average crystallites size from 5 μm to 3 μm in $(Cu_{0.75}Ag_{0.25})_7SiS_5I$-based ceramics.

The temperature dependences of the ionic and electronic components of electrical conductivity in the Arrhenius coordinates are presented in Fig. 7. It is ascertained that they are linear and described by the Arrhenius equation, which confirms the thermoactivating character of electrical conductivity. Using the linear part of temperature dependences, the activation energies of both ionic and electronic components of electrical conductivity were determined (Fig. 6b). It should be noted that dependence of activation energy of ionic conductivity for $(Cu_{0.75}Ag_{0.25})_7SiS_5I$-based ceramics is nonlinear (Fig. 6a), which is manifested in the reduction of activation energy in the context of the average crystallite size decrease from 12 μm down to 5 μm, while with a decrease of the average crystallite size from 5 μm down to 3 μm the activation energy tends to increase. Instead, the activation energy of electronic conductivity approximately linearly increases with decreasing the average crystallite size from 12 μm down to 3 μm (Fig. 6b).

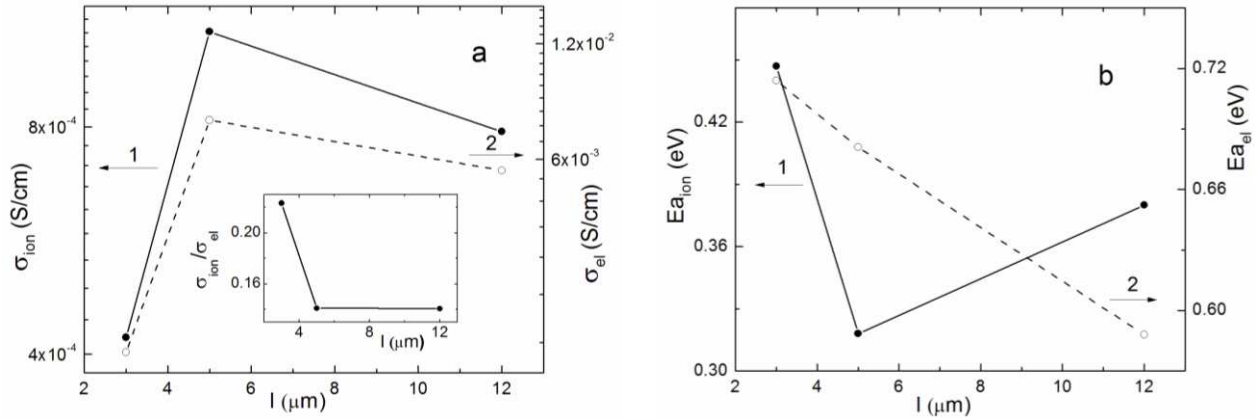*Studenyak I.P., Pogodin A.I., Shender I.A. et al. Structural and impedance studies of copper-enriched...*

263

Fig. 6. Temperature dependences of ionic (a) and electronic (b) components of electrical conductivity for $(Cu_{0.75}Ag_{0.25})_7SiS_5I$-based ceramics with different crystallite sizes: 12 μm (*1*), 5 μm (*2*), 3 μm (*3*).
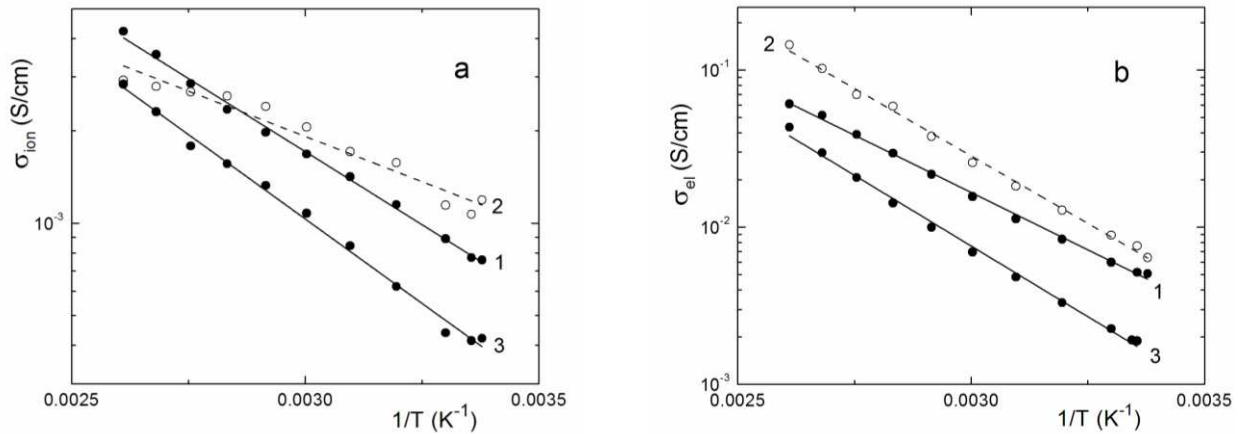

Fig. 7. (a) Dependences of ionic (*1*) and electronic (*2*) components of electrical conductivity at $T = 298$ K on the size of crystallites for $(Cu_{0.75}Ag_{0.25})_7SiS_5I$-based ceramics, the insert shows the dependence of the ratio of the conductivity components on the size of the crystallites. (b) Dependences of the activation energy inherent to the ionic (*1*) and electronic (*2*) components of electrical conductivity on the size of crystallites for $(Cu_{0.75}Ag_{0.25})_7SiS_5I$-based ceramics.

Finally, it should be noted that $(Cu_{0.75}Ag_{0.25})_7SiS_5I$-based ceramics are characterized by complicated and disordered micro- and macrostructure, which is associated with different size of crystallites (Fig. 3), their non-regular distribution, and complicate recrystallization process during sintering micro- and nanocrystalline powders. This process, first of all, includes the consolidation of crystallites due to the processes of solid-phase diffusion and, as a result, "dissolution" of smaller particles by larger ones – recrystallization, which is clearly visible according to the crystallite size distribution curve (Fig. 3) and provided microstructural research data. In the process of recrystallization, the emergence of microstructural inhomogeneities is inevitable, which contributes to the emergence of micro- and, consequently, macrodefects. This additionally leads to the appearance of internal stress of the ceramic material. Here we should also add a disordered crystal structure of $(Cu_{0.75}Ag_{0.25})_7SiS_5I$, caused by $Cu^+ \leftrightarrow Ag^+$ cationic substitution. This combination of above features in the final case leads to the change of the Nyquist plots for the samples with different average crystallite sizes

(Fig. 5) and causes the corresponding behavior of the total electrical conductivity (Fig. 4), its components (ionic and electronic conductivity) (Fig. 6), and is defined by the nature of thermoactivation behavior (Fig. 7) of $(Cu_{0.75}Ag_{0.25})_7SiS_5I$-based ceramics.

4. Conclusions

The copper-enriched $(Cu_{0.75}Ag_{0.25})_7SiS_5I$ solid solution was synthesized, then it was grinded into the micro- and nanopowders in an agate mortar and in a planetary ball mill, and further the obtained powders were pressed and sintered. The X-ray diffraction studies of the micro- and nanopowders have shown the lines broadening with decreasing the size of particles. From the micro- and nanopowders, the different types of $(Cu_{0.75}Ag_{0.25})_7SiS_5I$-based ceramics with the average crystallite sizes 3, 5 and 12 μm were produced. The obtained ceramic samples were investigated by microstructural analysis, which resulted in the dependences of size distribution and microstructure images of the samples surface.

Studenyak I.P., Pogodin A.I., Shender I.A. et al. Structural and impedance studies of copper-enriched…

Electrical conductivity studies for $(Cu_{0.75}Ag_{0.25})_7SiS_5I$-based ceramics were performed within the frequency range $10...2 \times 10^6$ Hz and temperature range 292...383 K. The Nyquist plots were analyzed using the electrode equivalent circuits. Being based on them, the ionic and electronic components of electrical conductivity were determined. It has been revealed that decrease of the average crystallite sizes from 12 µm down to 5 µm leads to the increase of both ionic and electronic components of electrical conductivity, while the further decrease from 5 µm down to 3 µm leads to the significant decrease of both components of electrical conductivity. At the same time, the ratio of ionic to electronic conductivity remains unchanged with decreasing the average crystallite size from 12 µm down to 5 µm and increases with the decrease of it from 5 µm down to 3 µm.

The temperature dependences of ionic and electronic components of electrical conductivity are linear in Arrhenius coordinates, which confirms the thermoactivating character of electrical conductivity. The complex and disordered micro- and macrostructure of $(Cu_{0.75}Ag_{0.25})_7SiS_5I$-based ceramics is related with the different sizes of crystallites, their non-regular distribution and complicated recrystallization process during sintering micro- and nanocrystalline powders.

References

1. Kuhs W.F., Nitsche R., Scheunemann K. The argyrodites – a new family of the tetrahedrally close-packed structures. *Mater. Res. Bull*. 1979. **14**, No 2. P. 241–248. https://doi.org/10.1016/0025-5408(79)90125-9.

2. Nilges T., Pfitzner A. A structural differentiation of quaternary copper argyrodites: Structure – property relations of high temperature ion conductors. *Z. Kristallogr*. 2005. **220**. P. 281–294. https://doi.org/10.1524/zkri.220.2.281.59142.

3. Laqibi M., Cros B., Peytavin S., Ribes M. New silver superionic conductors Ag_7XY_5Z (X = Si, Ge, Sn; Y = S, Se; Z = Cl, Br, I) – synthesis and electrical properties. *Solid State Ionics*. 1987. **23**. P. 21–26. https://doi.org/10.1016/0167-2738(87)90077-4.

4. Studenyak I.P., Pogodin A.I., Studenyak V.I., Izai V.Yu., Filep M.J., Kokhan O.P., Kranjčec M., Kúš P. Electrical properties of copper- and silver-containing superionic $(Cu_{1-x}Ag_x)_7SiS_5I$ mixed crystals with argyrodite structure. *Solid State Ionics*. 2020. **345**. P. 115183. https://doi.org/10.1016/j.ssi.2019.115183.

5. Orliukas A.F., Kazakevicius E., Kezionis A. *et al*. Preparation, electric conductivity and dielectrical properties of Cu_6PS_5I-based superionic composites. *Solid State Ionics*. 2009. **180**, No 2-3. P. 183–186. https://doi.org/10.1016/j.ssi.2008.12.005.

6. Studenyak I.P., Izai V.Yu., Studenyak V.I. *et al*. Influence of Cu_6PS_5I superionic nanoparticles on the dielectric properties of 6CB liquid crystal. *Liquid Crystals*. 2017. **44**, No 5. P. 897–903. https://doi.org/10.1080/02678292.2016.1254288.

7. Šalkus T., Kazakevičius E., Banys J. *et al*. Influence of grain size effect on electrical properties of Cu_6PS_5I superionic ceramics. *Solid State Ionics*. 2014. **262**. P. 597–600. https://doi.org/10.1016/j.ssi.2013.10.040.

8. Studenyak I.P., Kranjčec M., Izai V.Yu. *et al*. Structural and temperature-related disordering studies of Cu_6PS_5I amorphous thin films. *Thin Solid Films*. 2012. **520**, No 6. P. 1729–1733. https://doi.org/10.1016/j.tsf.2011.08.043.

9. Fernao Pires V., Romero-Cadaval E., Vinnikov D. *et al*. Power converter interfaces for electrochemical energy storage systems – A review. *Energy Conversion and Management*. 2014. **86**. P. 453–475. https://doi.org/10.1016/j.enconman.2014.05.003.

10. Wu Z., Xie Z., Yoshida A. *et al*. Utmost limits of various solid electrolytes in all-solid-state lithium batteries: A critical review. *Renewable and Sustainable Energy Reviews*. 2019. **109**. P. 367–385. https://doi.org/10.1016/j.rser.2019.04.035.

11. Goodenough J.B., Park K.-S. The Li-ion rechargeable battery: a perspective. *J. Am. Chem. Soc*. 2013. **135**, No 4. P. 1167–1176. https://doi.org/10.1021/ja3091438.

12. Wen J., Yu Y., Chen C. A review on lithium-ion batteries safety issues: Existing problems and possible solutions. *Mater. Exp*. 2012. **2**, No 3. P. 197–212. https://doi.org/10.1166/mex.2012.1075.

13. Fergus J.W. Ceramic and polymeric solid electrolytes for lithium-ion batteries. *J. Power Sources*. 2010. **195**, No 15. P. 4554–4569. https://doi.org/10.1016/j.jpowsour.2010.01.076.

14. Zhang Z., Zhang Q., Ren C. *et al*. A ceramic/polymer composite solid electrolyte for sodium batteries. *J. Mater. Chem*. A. 2016. **4**, No 41. P. 15823–15828. https://doi.org/10.1039/C6TA07590H.

15. Urusov V.S. *Theoretical Crystallochemistry*. Moscow: MGU, 1987 (in Russian).

16. Rietveld H.M. A profile refinement method for nuclear and magnetic structures. *J. Appl. Crystallogr*. 1969. **2**, No 2. P. 65–71. http://dx.doi.org/10.1107/S0021889869006558.

17. McCusker L.B., Von Dreele R.B., Cox D.E., Louër D., Scardi P. Rietveld refinement guidelines. *J. Appl. Crystallogr*. 1999. **32**, No 1. P. 36–50. https://doi.org/10.1107/S0021889898009856.

18. Altomare A., Burla M.C., Camalli M. *et al*. EXPO: a program for full powder pattern decomposition and crystal structure solution. *J. Appl. Crystallogr*. 1999. **32**, No 2. P. 339–340. https://doi.org/10.1107/S0021889898007729.

19. Altomare A., Cuocci C., Giacovazzo C. *et al*. EXPO2013: a kit of tools for phasing crystal structures from powder data. *J. Appl. Crystallogr*. 2013. **46**, No 4. P. 1231–1235. https://doi.org/10.1107/S0021889813013113.

20. Momma K., Izumi F. VESTA 3 for three-dimensional visualization of crystal, volumetric and morphology data. *J. Appl. Crystallogr*. 2011. **44**. P. 1272–1276. https://doi.org/10.1107/S0021889811038970.

Studenyak I.P., Pogodin A.I., Shender I.A. et al. Structural and impedance studies of copper-enriched…

265

21. Ivanov-Schitz A.K., Murin I.V. *Solid State Ionics.* St.-Petersburg: Univ. Press, 2000 (in Russian).
22. Orazem M.E., Tribollet B. *Electrochemical Impedance Spectroscopy.* New Jersey: John Wiley & Sons, 2008.
23. Huggins R.A. Simple method to determine electronic and ionic components of the conductivity in mixed conductors a review. *Ionics.* 2002. **8**, No 3. P. 300–313. https://doi.org/10.1007/BF02376083.

Authors and CV

Ihor P. Studenyak, defended his Dr. Sc. degree in Physics and Mathematics in 2003 and became full professor in 2004. Vice-rector for research at the Uzhhorod National University, Ukraine. Authored over 200 publications, 120 patents, 15 textbooks. The area of his scientific interests includes physical properties of semiconductors, ferroics and superionic conductors.
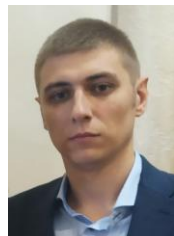
Artem I. Pogodin defended his PhD thesis in inorganic chemistry in 2016. Senior researcher at the Uzhhorod National University. Authored over 35 articles and 50 patents. The area of his scientific interests includes solid state chemistry, crystal growth, and materials science.

Iryna A. Shender, born in 1995. Currently she is PhD student at the Uzhhorod National University, Faculty of Physics. The area of her scientific interests is electrical and optical properties of superionic conductors.

Serhiy M. Bereznyuk, born in 1996. Currently he is PhD student at the Uzhhorod National University, Faculty of Physics. Authored of 1 publication and 3 patents. The area of scientific interests is electrical and optical properties of superionic conductors.

Mykhailo J. Filep, born in 1987, defended his PhD thesis in inorganic chemistry in 2015. Senior researcher at the Uzhhorod National University. Authored over 40 articles and 20 patents. The area of his scientific interests includes solid state chemistry and materials science.

Oleksandr P. Kokhan defended his PhD thesis in inorganic chemistry in 1996. Associate professor of Inorganic Chemistry department at the Uzhhorod National University. Authored over 80 articles and 40 patents. The area of his scientific interests includes inorganic chemistry, solid state chemistry, crystal growth, materials science.

Peter Kopčanský, Professor in solid state physics. Senior researcher of Institute of Experimental Physics, Slovak Academy of Sciences. Authored over 250 articles, 6 patents, 5 textbooks. The area of his scientific interests includes solid state physics, especially magnetism, transport properties in disordered systems, magnetic fluids, their magnetic and dielectric properties and composite systems with liquid crystals.

Структурні та імпедансні дослідження кераміки на основі збагаченого міддю $(Cu_{0.75}Ag_{0.25})_7SiS_5I$

І.П. Студеняк, А.І. Погодін, І.А. Шендер, С.М. Березнюк, М.Й. Філеп, О.П. Кохан, P. Корчанський

Анотація. Кераміку на основі збагаченого міддю $(Cu_{0.75}Ag_{0.25})_7SiS_5I$ отримано згідно з розробленими технологічними умовами з мікро- та нанопорошків шляхом пресування та спікання. Структурні дослідження на різних стадіях процесу підготовки зразків кераміки проведено за допомогою методу рентгенівської дифракції та мікроструктурного аналізу. Частотні та температурні залежності загальної електропровідності кераміки на основі $(Cu_{0.75}Ag_{0.25})_7SiS_5I$ було досліджено шляхом імпедансних вимірювань. З використанням діаграм Найквіста за допомогою електродних еквівалентних схем визначали іонні та електронні компоненти загальної електропровідності. Показано, що іонна та електронна електропровідності нелінійно залежать від середнього розміру кристалітів кераміки на основі $(Cu_{0.75}Ag_{0.25})_7SiS_5I$.

Ключові слова: аргіродит, суперіонний провідник, кераміка, іонна провідність, енергія активації.

Studenyak I.P., Pogodin A.I., Shender I.A. et al. Structural and impedance studies of copper-enriched…

266